Luminescent vapochromic single crystal to single crystal transition in one-dimensional coordination polymer featuring the first Cu(i) dimer bridged by an aqua ligand

Sloane Evariste, Ali Moustafa Khalil, Sebastien Kerneis, Chendong Xu, Guillaume Calvez, Karine Costuas, Christophe Lescop

Luminescent vapochromic single crystal to single crystal transition in one-dimensional coordination polymer featuring the first Cu(I) dimer bridged by an aqua ligand.

Sloane Evariste, Ali Moustafa Khalil, Sebastien Kerneis, Chendong Xu, Guillaume Calvez,* Karine Costuas* and Christophe Lescop*

The reaction of the pre-assembled bimetallic Cu(I) $[Cu_2(\mu_2\text{-dppm})_2]^{2+}$ fragment with the ligand 1,4-dicyanobenzene **B_0** in non-distillated CH_2Cl_2 allows the characterisation of an unexpected one-dimensional coordination polymer **D**, while no reaction occurs when dry CH_2Cl_2 is used as solvent. X-ray crystal structure resolution performed on air-stable single crystals of **D** reveals that this coordination polymer contains the first-ever reported bridging aqua ligand coordinated on Cu(I) bimetallic units connected by **B_0** ligands within zig-zag chains. Consequently, **D** can be obtained in a very good yield when the synthesis is conducted in dry CH_2Cl_2 in which water is added as reactant in excess. In the solid state at room temperature under UV lamp excitation, **D** present a blue-cyan eye-perceived luminescence that contrats with the green-yellow eye-perceived luminescence emitted by the single crystals of **D** in the crystallisation solution. Related to this property, a reversible luminescent vapochromic behaviour is highlighted upon exposure of dry single crystals of **D** to vapors of CH_2Cl_2, EtOH, CH_3NO_2 and THF solvents. X-ray crystal structure resolution analysis revealed that this vapochromic response occurs via single crystal to single crystal transitions along which the volatile solvent molecules are uptake in the very low porous dry single crystals of **D**, leading to the formation of one-dimensionnal channels of included solvent molecules that are mobile in the crystalline solids at room temperature. Detailed temperature dependent photophysical studies suggest that this mobility impacts the relaxation processes within these molecular solids, originating these luminescence vapochromic effects. They also highlight the complexity of the relaxation processes that can take place in such heteroleptic polymetallic Cu(I) supramolecular assemblies that , in contrast, are based on highly easy, affordable and quick synthetic procedure

Introduction

The design and the study of luminescent material based on coordination metal complexes attract a great attention due to the manifold fields of application that these derivatives can address.[1] In this field, Cu(I) coordination complexes supply a very fertile environment for impressive developments because of the fascinating and various photophysical properties they can exhibit.[1a,2] While these derivatives focus currently great attention for the preparation and study of innovative emitters in OLEDs,[2a] they deserve also interest as new sources of stimuli responsive multifunctional luminescent materials.[2b] Indeed, the large flexibility and lability of Cu(I) ion coordination sphere render the gross conformation of Cu(I) species potentially very sensitive to external stimuli, which concomitantly induces alteration of their photophysical properties. Therefore, Cu(I)-based luminophors present multiple and original facets[3] (such as thermochromic and vapochromic luminescence) that are of great interest in various fields of applications such as sensoring and detection of volatile harmful chemical substances or non-destructive testing of materials.

Regarding specifically Cu(I)-based solid-state vapochromic luminescent luminophores, it is assumed that the origin of their vapochromic properties is due either to structural transitions occurring along desorption/adsorption processes of volatile molecules within porous Cu(I)-based materials,[3a,b] or to reversible coordination/de-coordination of these molecules[3c] on coordinatively-unsaturated Cu(I) metal centers. In all cases, these events impact reversibly the electronic structure of the assemblies in their ground and photo-excited states, inducing the luminescence vapochromic effect.

Among the manifold Cu(I) complexes reported so far, there are remarkably few stable Cu(I) complexes described in which the metal center is coordinated to a terminal aqua ligand.[4] Herein,

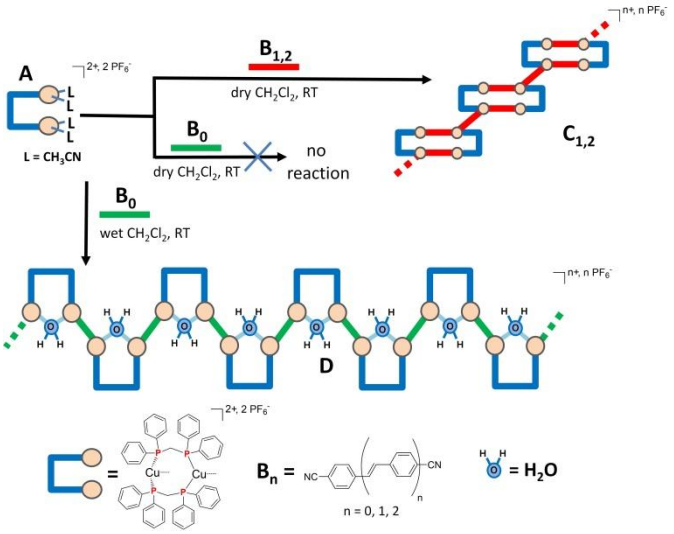

Scheme 1 Synthesis of derivative $\mathbf{C_{1,2}}$[5] and **D**.

we report the preparation of a new luminescent one-dimensional coordination polymer (1D-CP) **D** bearing the first semi-bridging aqua ligand coordinated to a Cu(I) ions bimetallic unit reported so far. This polymer presents vapochromic solid-state luminescence properties that are related to single crystal to single crystal (SC-SC) phase transition induced by the reversible incorporation of volatile solvent molecules within the crystalline network. The luminescence vapochromic effect is related to a molecular motion that takes place within the 1D-CP's backbone in the solid state, activated by the volatile molecule uptake. Its

amplitude depends on both the temperature and the nature of the solvent molecules introduced.

Results and discussion

We have previously shown that the pre-assembled bimetallic $[Cu_2(\mu_2\text{-dppm})_2(CH_3CN)_4](PF_6)_2$ complex **A** reacts at room temperature (RT) with homoditopic cyano-capped oligophenylvinylene-based linkers $\mathbf{B_{1,2}}$ to afford in good yields single crystals of the 1D-CPs $\mathbf{C_{1,2}}$.[5] Their supramolecular backbones lies on the connection of tetrametallic π-stacked compact metallacycles[6] by ditopic linkers $\mathbf{B_{1,2}}$ (Scheme 1). These reactions can be easily conducted either using anhydrous or non-distillated CH_2Cl_2 as solvent without changes in the reaction outcomes. However, when a similar procedure is applied in anhydrous CH_2Cl_2 using the shorter linker 1,4-dicyanobenzene $\mathbf{B_0}$, no reaction product can be isolated and the mother solution stays clear upon pentane vapor diffusion for several months. Interestingly, when non-distillated CH_2Cl_2 is used, crystallization experiments allow obtaining a few colorless single crystals after one week.[7] Conversely to the crystals of $\mathbf{C_{1,2}}$ that collapsed immediately once removed from the mother solution due to the loss of included CH_2Cl_2 solvent molecules,[5] these colorless crystals keep their single crystal integrity after being collected, dried and stored at room

Fig. 1. a) Views of the molecular X-ray structures of derivative $\mathbf{D_{dry}}$: a) repetition unit b) fragment of the 1D-CP zig-zag chain, c) location of the PF_6^- anions and the H-F short contact interactions (black doted lines) between the PF_6^- and the aqua ligand.

temperature (RT), affording the species $\mathbf{D_{dry}}$. X-ray diffraction studies[7] performed at 150 K on these single crystals revealed the formation of a new 1D-CP $\mathbf{D_{dry}}$ (scheme 1) whose scaffold is different from those of $\mathbf{C_{1,2}}$. The compound $\mathbf{D_{dry}}$ crystallizes in the $P2_1/c$ space group of the monoclinic system. This new 1D-CP displays a zig-zag geometry that propagates parallel to the c crystallography axis (Fig. 1). Its asymmetric unit contains a $[Cu_2(\mu_2\text{-dppm})_2]$ unit, a 1,4-dicyanobenzene ligand $\mathbf{B_0}$, a semi-bridging coordinated water molecule and two hexafluorophosphate counter-anions. The water molecule acts as a μ-1,2κ-O semi-bridging aqua ligand (d(O-Cu) = 2.222(3) and 2.339(4) Å, the latter value being slightly shorter than the sum of the ionic radius of Cu(I) and O^{2-} centers (2.36 Å)) supplying the first example reported so far of such bridging coordination mode for an aqua ligand on Cu(I) metal centers. The metric parameters of the $[Cu_2(\mu_2\text{-dppm})_2]$ units are very similar to those observed usually for such fragment.[7] The intermetallic distance (3.1300(9) Å) is too large for cuprophilic interactions at the ground state, but is shorter than the Cu-Cu distances observed within the $[Cu_2(\mu_2\text{-dppm})_2]$ units of the 1D-CPs $\mathbf{C_{1,2}}$ (> 3.2 Å). The backbone of this 1D-CP (Fig. 1) is based on $[Cu_2(\mu_2\text{-dppm})_2(\mu_2\text{-OH}_2)]$ fragments connected to a ligand $\mathbf{B_0}$ that acts as a ditopic linker between two neighboring bimetallic Cu(I) units in *trans*-orientation relatively to each other. The coordination angle between the Cu(I) metal centers and the nitrile moieties deviate notably from the linearity (Cu-N≡C = 154.6(4)° and 158.6(4)°). In the bulk crystalline solid state of $\mathbf{D_{dry}}$, the 1D-CPs are parallel and are slightly nested inside each other (Fig. 2a) via weak π-CH interactions involving the phenyl rings of the dppm ligands. These 1D-chains are also connected via the hexafluorophosphate anions that share H···F interactions with the coordinated water molecules (Fig. 1c) and π···F interactions

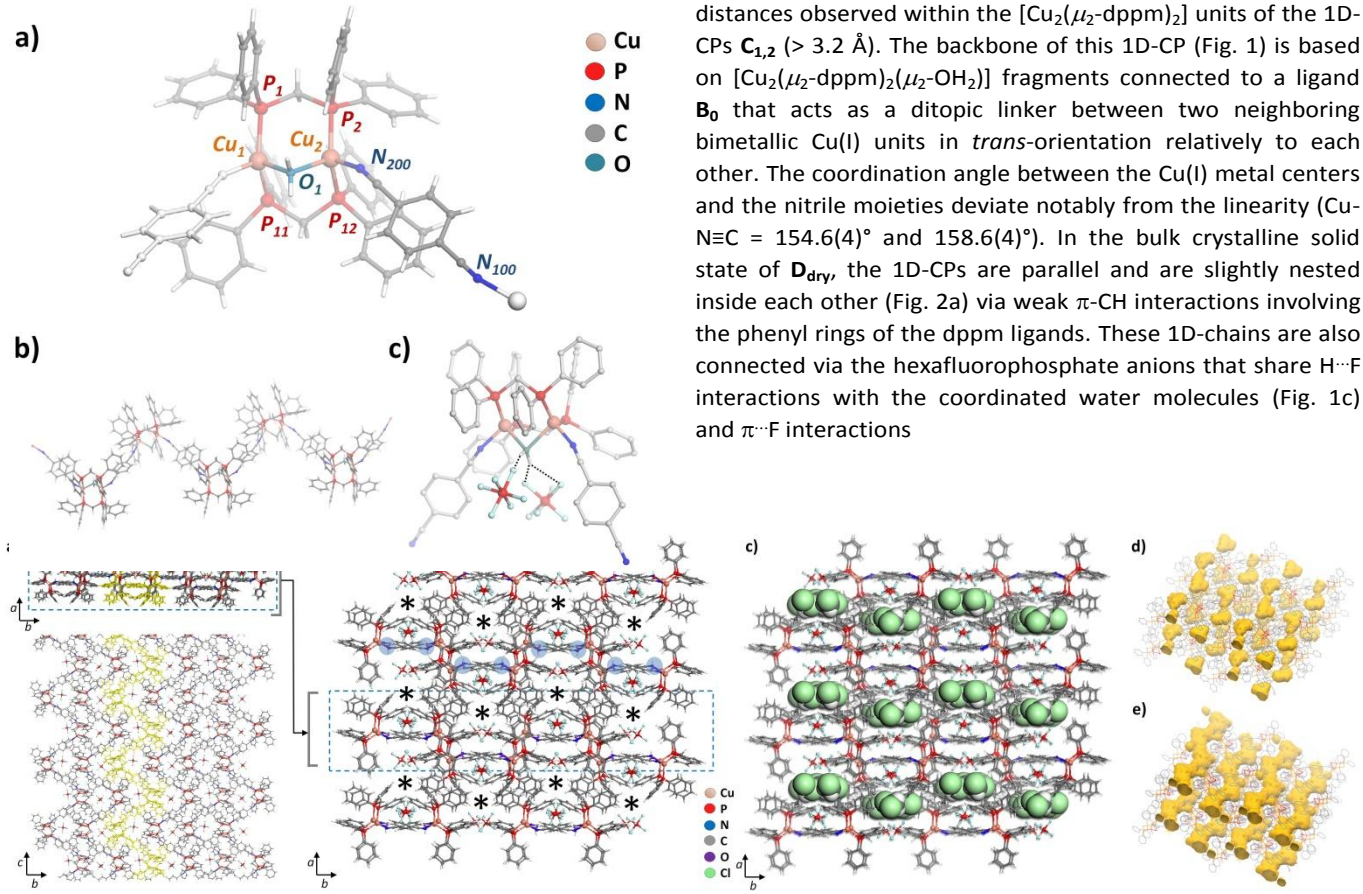

Fig. 2. a) ''side'' and ''top'' view of the two dimensional layers made by the imbricated 1D-CPs in $\mathbf{D_{dry}}$ (one independent 1D-CP is highlighted in yellow; the backbones of the 1D-CP are shown in the stick and ball representation mode); b) stacking mode of these layers (one layer is framed by the dotted line, location of the small voids are highlighted by black asterisk, location of the

aqua ligands in one layer highlighted with blue circles); c) view of the crystal structure of $\mathbf{D_{CH2Cl2}}$ (included CH_2Cl_2 molecules are represented in the CPK representation mode); representation of the volume d) of the cavities in $\mathbf{D_{dry}}$ and e) occupied by the solvent molecules in $\mathbf{D_{CH2Cl2}}$ (a spherical probe radius of 1.2 Å was chosen in order to clearly visualize these volumes and their different morphologies).

with the phenyl rings of the dppm or $\mathbf{B_0}$ ligands. As a result of these interchain interactions, imbrication of the neighboring 1D-CPs results in the formation of bi-dimensional (2D) layers (Fig. 2a) that stack perpendicularly to the *a* axis (Fig. 2b). Finally, between these sheets, no residual electronic density is observed revealing the absence of included solvent molecules in these single crystals. Nevertheless, it is important to note that small and isolated voids of 113 $Å^3$ (ca. 1.8 % of the unit cell volume)[8] are observed between these layers (Fig. 2b,d).

The 1D-CP $\mathbf{D_{dry}}$ is the first derivative reported so far in which two Cu(I) metal centres are bridged by an aqua ligand.[9] Very likely, these aqua ligands are supplied by the residual water molecules present in non-distillated CH_2Cl_2 solvent. While Cu(I) complexes bearing a coordinated terminal aqua ligand are scarce,[4] suggesting a low affinity of water molecules for Cu(I) ions in agreement with their respective Pearson's hard base and soft acid characters, the presence of water in this synthesis revealed to be crucial to obtain $\mathbf{D_{dry}}$. Indeed, while experiments conducted with anhydrous CH_2Cl_2 did not afford any crystals, when the reaction was performed using anhydrous CH_2Cl_2 as solvent in which a drop of water was added (Scheme 1), supplying water ligand molecules as reagent in excess, the preparation of derivative $\mathbf{D_{dry}}$ was very significantly improved allowing to collect this 1D-CP after crystallization in a good yield (ca. 80%).

In most of the few cases published so far,[4] Cu(I) complexes bearing coordinated water molecules are not described as being emissive in the solid state upon UV-vis light excitation. Yet, Kato *et al.* described recently the two first RT solid state luminescent Cu(I) derivatives bearing terminal aqua ligands,[4a] suggesting that the coordination of a water molecule on a Cu(I) center is not always detrimental regarding solid-state luminescence properties. In agreement with this assumption, we observed that the colorless polycrystalline samples of $\mathbf{D_{dry}}$ emit, under UV-Vis light excitation (λ_{ex} = 365 nm), an eye-perceived blue-cyan luminescence. Interestingly, we also observed that, before being removed from their crystallization solution, the single crystals grown emit under the same UV-light excitation a markedly different eye-perceived green-yellow luminescence. In addition, single crystal of $\mathbf{D_{dry}}$ exposed under air to CH_2Cl_2 vapors (affording $\mathbf{D_{CH2Cl2}}$ single crystals) instantaneously switched their solid-state eye-perceived blue-cyan emission to an eye-perceived green-yellow luminescence of a similar color than observed when crystals are maintained in the crystallization solution. The initial blue-cyan luminescence is recovered once the CH_2Cl_2 vapor source is removed, indicating a reversible vapochromic luminescence response of $\mathbf{D_{dry}}$ toward CH_2Cl_2 vapors. In order to get structural insights about the origin of such luminescence vapochromism properties, single-crystals of $\mathbf{D_{CH2Cl2}}$ lying in an atmosphere saturated with CH_2Cl_2 vapors were coated in paratone oil (in which they were still emitting an eye-perceived green-yellow luminescence upon UV-excitation) and submitted to X-ray diffraction single-crystal analysis at 150 K. It revealed that $\mathbf{D_{CH2Cl2}}$ kept single crystal integrity during the process, bearing as $\mathbf{D_{dry}}$, a $P2_1/c$ monoclinic unit cell. Yet, its unit cell volume is larger ($\mathbf{D_{CH2Cl2}}$: ca. 6340 $Å^3$, $\mathbf{D_{dry}}$: ca. 6082 $Å^3$), mostly due to an increase of the *a* parameter value ($\mathbf{D_{CH2Cl2}}$: 13.972(2) Å; $\mathbf{D_{dry}}$: 13.2578(6) Å), the other unit cell parameters being only very moderately altered (Table S1). X-ray single crystal structure resolution revealed that $\mathbf{D_{CH2Cl2}}$ composition is very similar of the one of $\mathbf{D_{dry}}$, being based on a zig-zag 1D-CP with a dicationic $[Cu_2(\mu_2\text{-dppm})_2(\mu_2\text{-}OH_2)(\mathbf{B_0})](PF_6)_2$ repetition unit, but very importantly, two disordered included CH_2Cl_2 solvent molecules are additionally found in the unit cell of $\mathbf{D_{CH2Cl2}}$ (Fig. 2c). Similarly to $\mathbf{D_{dry}}$, the 1D-CPs in $\mathbf{D_{CH2Cl2}}$ are imbricated affording 2D layers that stack perpendicular to the *a* axis. The metric parameters observed for the asymmetric unit of $\mathbf{D_{dry}}$ and $\mathbf{D_{CH2Cl2}}$ are very similar (for example, d(Cu(1)-Cu(2): 3.130(2) Å ($\mathbf{D_{dry}}$) and 3.132(3) Å ($\mathbf{D_{CH2Cl2}}$); (Cu_1-O_1-Cu_2) angle: 86.42(10)° ($\mathbf{D_{dry}}$) and 86.2(2)° ($\mathbf{D_{CH2Cl2}}$)) and the gross geometry of the 1D-CPs are very comparable. Nevertheless, in

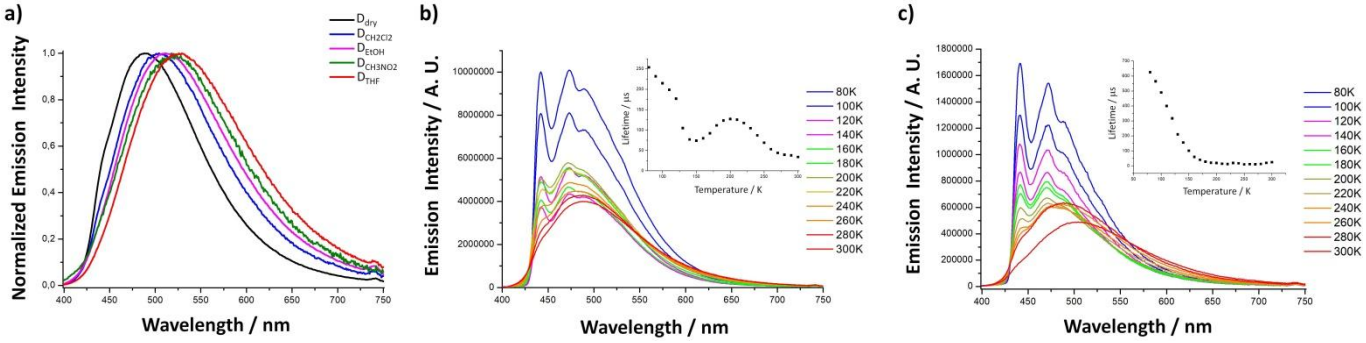

Fig. 3. a) Normalized solid-state emission spectra of $\mathbf{D_{dry}}$, $\mathbf{D_{CH2Cl2}}$, $\mathbf{D_{EtOH}}$, $\mathbf{D_{CH3NO2}}$ and $\mathbf{D_{THF}}$ at 300 K upon excitation at 370 nm; b) Solid-state emission spectra of $\mathbf{D_{dry}}$ at temperatures between 80 K and 300 K upon excitation at 370 nm; insert: plot of emission decay lifetime against temperature (80 K to 300 K); c) Solid-state emission spectra of $\mathbf{D_{CH2Cl2}}$ at temperatures between 80 K and 300 K upon excitation at 370 nm; insert: plot of emission decay lifetime against temperature (80 K to 300 K).

the case of $\mathbf{D_{CH2Cl2}}$ the 2D layers are separated by larger intermolecular distances corresponding to the increase of the value of the *a* parameter found for each unit cell. The CH_2Cl_2 molecules found in $\mathbf{D_{CH2Cl2}}$ are located between these 2D layers (Fig. 2c), occupying formally at the same position than the voids found in the solid-state structure of $\mathbf{D_{dry}}$ (Fig. 2b and 2c). Yet, the volume occupied by these solvent molecules (Fig. 2e) describes in $\mathbf{D_{CH2Cl2}}$ infinite zig-zag 1D-channels (corresponding to ca. 2.7 % of the unit cell volume)[8] that propagate parallel to the *c* crystallography axis. It is important to stress that along these cavities, one phenyl ring of one of the two dppm ligands is found disordered over two positions (see Fig. S3) while no disorder is identified on any fragment of the 1D-CP backbone of the non-solvated structure $\mathbf{D_{dry}}$. This disordered phenyl ring is closely located to the included CH_2Cl_2 solvent molecules. Finally, in order to allow conducting a comparative structure/photophysical behavior analysis of the thermal variation of the properties of $\mathbf{D_{dry}}$ and $\mathbf{D_{CH2Cl2}}$ (*vide infra*), temperature dependent X-ray structural study of these two phases was performed. It revealed that both crystals $\mathbf{D_{dry}}$ and $\mathbf{D_{CH2Cl2}}$ present only a very moderate and progressive shrinkage of the unit cell volume from 250 K to 150 K (*ca.* 1.5 % and 1.8 % volume contraction, respectively). This indicates that the solid state structural metric data of these 1D-CPs, established at 150 K, are kept mostly unchanged as temperature changes without occurrence of significant phase transition (*vide infra*). A green-yellow luminescent single crystal freshly collected in the CH_2Cl_2/pentane crystallization solution was also submitted to X-ray diffraction analyses. It revealed that this compound is isostructural of those preliminary dried ($\mathbf{D_{dry}}$) and subsequently submitted to CH_2Cl_2 vapors ($\mathbf{D_{CH2Cl2}}$). Therefore, CH_2Cl_2 solvent molecules are initially included in the single-crystals along the crystallization process. Once the single-crystals are removed from the mother solution, they release very rapidly their solvent molecules without loss of crystallinity, affording the blue-cyan luminophore $\mathbf{D_{dry}}$.

In the solid state at RT, $\mathbf{D_{dry}}$ exhibits a strong and broad absorption band (Fig. S15) in the near UV region typical of π-π* transition centered on the aromatic rings of dppm and $\mathbf{B_0}$ ligands. The TD-DFT calculations[7] revealed that they are corresponding to $[Cu_2(\mu_2\text{-dppm})_2]$ fragment to π*-dicyano-benzene charge transfer excitations. In its emission spectrum, $\mathbf{D_{dry}}$ displays under excitation at 370 nm at 300 K a broad featureless band centered at λ_{max} = 486 nm (Fig. 3a). [7,10] The average emissive lifetime τ is 38 μs and an emission RT quantum yield (EQY) is 20 %. Such band is in agreement with the solid-state eye-perceived blue-cyan luminescence observed arising from the single-crystals of $\mathbf{D_{dry}}$ upon UV-light irradiation. The RT solid-state absorption spectrum of $\mathbf{D_{CH2Cl2}}$ is very similar to the one of $\mathbf{D_{dry}}$ (Fig. S16) but its RT solid-state emission spectrum measured under excitation at 370 nm presents a broad featureless band centered at 502 nm (Fig. 3a), being significantly red-shifted regarding the band observed for $\mathbf{D_{dry}}$ (λ_{max} = 486 nm). This bathochromic shift is accompanied by a decrease of both the RT emissive lifetime and the EQY, being respectively of 13 μs and 7 %. The origin of red-shift observed in the emission spectra of $\mathbf{D_{CH2Cl2}}$ compared to $\mathbf{D_{dry}}$ is unclear and difficult to be rationalized considering the close similarities of the solid-state parameters established for both derivatives. Therefore, to get more insights about the emission properties of $\mathbf{D_{dry}}$ and $\mathbf{D_{CH2Cl2}}$, temperature dependent photophysical characterizations were conducted for both phases upon temperature cooling from 300 K to 80 K. In the emission spectra of $\mathbf{D_{dry}}$ under excitation at 370 nm,[11] a gradual and very moderate blue-shift (Fig. 3b) of the large band observed at 300 K (λ_{max} = 486 nm) first occurs up to 260 K (λ_{max} = 482 nm), together with a slight increase of the signal intensity. From 260 K to 200 K, this intensity enhancement continues but is accompanied by a progressive structuration of the emission band. It yields at 200 K a large emission band bearing clearly two maxima centered at 443 and 474 nm and a shoulder at 490 nm, revealing the rise of a vibronic progression very likely assignable to ligand-centered transitions involving the 1,4-dicyanobenzene $\mathbf{B_0}$ connecting ligand. Indeed, such a vibronic structuration has never been observed in the thermal variation of related luminescent polymetallic supramolecular assemblies based on the $[Cu_2(\mu_2\text{-dppm})_2]$ moiety and cyano-based inorganic ligands.[12] Upon cooling down to 140 K, this vibronic progression becomes more defined but, quite unexpectively, a decrease of the intensity of the whole spectrum is observed. Finally, between 140 K and 80 K, the intensity of the signal increases continuously while the band shape is not significantly altered. The thermal variation of the average emission decay lifetime τ of $\mathbf{D_{dry}}$ (λ_{ex} = 370 nm, Fig. 3b) displays a very unusual profile.[13] Indeed, a constant increase is first observed from 300 K (τ = 38 μs) to 200 K (τ = 128 μs) but then occurs a surprising decay until 150 K (τ = 72 μs). Finally, the value of τ increases again as the temperature decreases and reaches 255 μs at 80 K. By comparing these two thermal dependencies, it is possible to highlight a correlation between the unusual behaviors observed in the luminescence properties of $\mathbf{D_{dry}}$. Hence, the intensity decrease of the emission spectra upon cooling between 200 K and 140 K (coming together with the concomitant increase of the vibronic progression) occurs in the same temperature window than the drop of the average emission decay lifetime τ. Very likely, these features witness

Table 1. Photophysical data (λ_{ex} = 370 nm) for derivatives $\mathbf{D_{dry}}$, $\mathbf{D_{CH2Cl2}}$, $\mathbf{D_{CH3NO2}}$, $\mathbf{D_{THF}}$ and $\mathbf{D_{EtOH}}$ at 298 K in the solid state.

	λ_{em} (nm)[a]	Φ_{em}	τ_{obs} (µs)[a]	k_r (s^{-1})[b]	k_{nr} (s^{-1})[c]
$\mathbf{D_{dry}}$	486 (443,474)	20	38 (255)	$5.3*10^3$	$2.1*10^4$
$\mathbf{D_{CH2Cl2}}$	502 (442,473)	7	13 (625)	$5.4*10^3$	$7.2*10^4$
$\mathbf{D_{CH3NO2}}$	522 (438, 469)	7	8 (430)	$8.7*10^3$	$1.2*10^5$
$\mathbf{D_{THF}}$	528 (437, 468)	7	12 (692)	$5.8*10^3$	$7.7*10^4$
$\mathbf{D_{EtOH}}$	512 (442 , 471 , 488	7	3 (62)	$2.3*10^4$	$3.1*10^5$

[a] Data recorded at 80 K are given in parentheses; [b] $k_r = \Phi_{em}/\tau_{obs}$; [c] $k_{nr} = (1-\Phi_{em})/\tau_{obs}$.

that competitive temperature-dependent relaxation pathways operate in the photophysical processes lying in $\mathbf{D_{dry}}$. Concerning the temperature dependence of the photophysical properties of $\mathbf{D_{CH2Cl2}}$, its emission spectra present upon cooling from 300 K (λ_{max} = 502 nm) to 260 K a significant hypsochromic shift (Fig. 3c) accompanied by a moderate increase in the intensity signal leading at 260 K to a large band centrered at λ_{max} = 485 nm. Below 260 K, while no spectral shift is observed, a continuous and progressive enhancement of the spectra intensity occurs together with a net structuration of the emission band. It results at 80 K in an emission spectrum bearing a signal with a clear vibronic progression associated with two maxima centered at 442 nm and 473 nm and a shoulder at 490 nm. Upon cooling the average emission decay lifetime τ of $\mathbf{D_{CH2Cl2}}$ (λ_{ex} = 370 nm, Fig. 3c) is kept constant from 300 K to 180 K (τ, ca. 20 μs) then it gradually increases until 80 K to reach the value of τ = 625 μs.

The solid-state emission behaviors of Cu(I)-based luminescent derivatives are characterized by the large diversity of the radiative relaxation processes involved, including for instance competitive temperature-dependant relaxation processes between different triplet states and Thermally Activated Delayed Fluorescence (TADF).[2,14] In the latter case, the thermal population of the lowest energy excited singlet state from the lowest energy triplet excited state occurs, inducing fast and efficient radiative relaxation to the ground state and remarkable RT solid-state luminescence properties. Considering the overall temperature-dependent data collected for the photophysical properties of the two 1D-CPs phases $\mathbf{D_{dry}}$ and $\mathbf{D_{CH2Cl2}}$, it is very likely that several temperature-dependant relaxation pathways involving different low energy singlet and triplet states are operant, implying competitive effects. This account in particular for the unusual behaviour of the photophysical parameters of $\mathbf{D_{dry}}$ between RT and 100 K (Fig. 3b). Indeed, this supports the hypothesis of a switch between at least two possible operating radiative relaxation processes. Tentatively, the photophysical behaviour of $\mathbf{D_{dry}}$ can be associated with a high temperature regime typical of a ^{3}MLCT phosphorescence on the basis of its k_r radiative rate constant value (Table 1) and a low temperature metal-perturbed $^3\pi$-π^* phosphorescence relaxation process mainly centered on the 1,4-dicyanobenzene $\mathbf{B_0}$ connecting ligands.[15]

The high temperature large unresolved bands observed in the emission spectra for $\mathbf{D_{dry}}$ and the high temperature thermal variation (between 300 K and 200 K) of its emission decay lifetime resemble significantly those previously reported for several luminescent Cu(I) polymetallic assemblies based on the [$Cu_2(\mu^2$-dppm$)_2$] unit and metallacyano ligands.[12a-c] In these derivatives, the large emission bands observed at RT are typical of metal-to-ligand charge transfer (MLCT) involving electronic densities at the cyano-based building blocks and the dppm ligands. In the case of the RT photophysical beahevior of $\mathbf{D_{dry}}$, the k_r radiative rate constant value is in favour of a purely ^{3}MLCT phosphorescence in which the high temperature large emission bands can be assigned radiative processes involving electronic densities located mostly on the 1,4-dicyanobenzene $\mathbf{B_0}$ ligands (also supported by the $S_0 \rightarrow S_1$/ and electronic density changes and their triplet counterpart $S_0 \rightarrow T_5/T_6$ shown in Fig. S18). Conversely, the low temperature emission spectra recorded for $\mathbf{D_{dry}}$ (Fig. 3b) can be assigned to phosphorescence from metal-perturbed $^3\pi$-π^* transitions centered on the 1,4-dicyanobenzene $\mathbf{B_0}$ connecting ligands in agreement with the nature of the calculated lowest vertical triplet states (Fig. S18). The longer values of the decay lifetimes and the vibronic structuration of the band observed at low temperature support such assumption of $\mathbf{B_0}$ ligand-centered $^3\pi$-π^* phosphorescence (Fig. 3b). Between ca. 250 K and ca. 100 K, both processes might be operant and compete, leading to the unusual thermal alteration of the photophysical parameters observed. It is worth noting that only a minor contribution of the semi-bridging aqua ligand is observed in the electronic excitation process on the basis of computational calculations (Fig. S18).[7] Therefore, this bridging aqua ligand, while playing a fundamental structurating role by promoting the formation of this unique 1D-CP network, is almost not involved in the relaxation processes governing the original photophysical properties observed, avoiding consequently the communly observed luminescence quenching effect of coordinated water molecules.

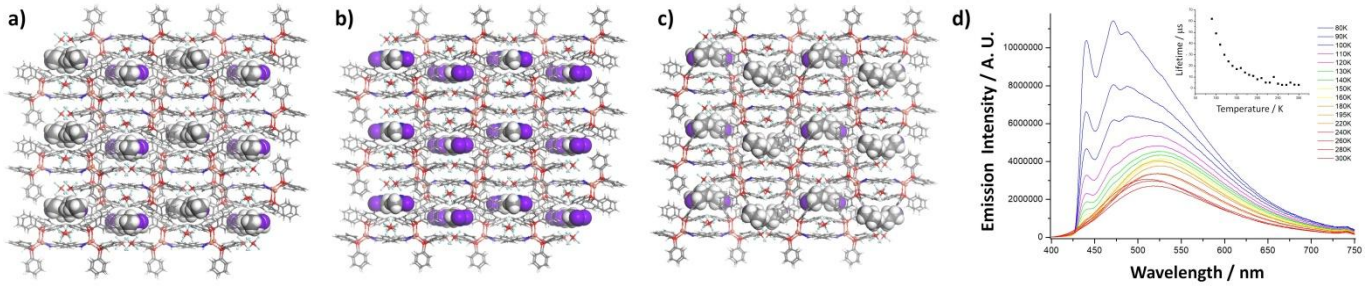

Fig. 4. Views of the X-ray structures of the derivatives a) $\mathbf{D_{EtOH}}$, b) $\mathbf{D_{CH3NO2}}$ and c) $\mathbf{D_{THF}}$; the backbones of the 1D-CP are shown in the stick and ball representation mode while the included solvent molecules are shown in the CPK representation mode; d) Solid-state emission spectra of $\mathbf{D_{EtOH}}$ at temperatures between 80 K and 300 K upon excitation at 370 nm; insert: plot of emission decay lifetime against temperature (80 K to 300 K).

The low temperature photophysical data recorded for $\mathbf{D_{dry}}$ and $\mathbf{D_{CH2Cl2}}$ (Fig. 3b and 3c) are comparable, despite slight differences in relative intensities at the different maxima in the emission spectra and longer average emission decay lifetime for $\mathbf{D_{CH2Cl2}}$. This suggests that the radiative relaxations rely on the similar $^3\pi$-π^* ligand-centered phosphorescence mechanism for both phases at these temperatures. The RT temperature k_r radiative rate constant value (Table 1) supports at high temperature also a ^{3}MLCT phosphorescence.[15] The differences accounting for the vapochromic behaviour can be related with the significantly different RT k_{nr} non-radiative rate constant values of $\mathbf{D_{dry}}$ and $\mathbf{D_{CH2Cl2}}$ (Table 1). Yet, the thermal variation of the emission decay lifetime for $\mathbf{D_{CH2Cl2}}$ (Fig. 3c) does not present the unusual profile recorded for $\mathbf{D_{dry}}$ (Fig. 3b), which likely is due to the largest difference in energy of ^{3}MLCT and $^3\pi$-π^* level in the less constrained $\mathbf{D_{CH2Cl2}}$ system. This is in spite of the fact that $\mathbf{D_{dry}}$ and $\mathbf{D_{CH2Cl2}}$ present similar 1D-CPs supramolecular architectures. Importantly, we mentioned that the inclusion of CH_2Cl_2 molecules in the single crystals of $\mathbf{D_{CH2Cl2}}$ is associated with the observation of a disorder at one phenyl ring of one dppm ligand in its low temperature X-ray single crystals structure. One can figure out that, in the high temperature regime, these included solvent molecules are mobile within the single crystals. This induces a molecular motion of the phenyl ring located in close vicinity of these mobile included solvent molecules and causes the disorder observed for this phenyl ring in the low temperature (150 K) X-ray structure of $\mathbf{D_{CH2Cl2}}$, a temperature at which this mobility is ''frozen'' at different positions. In turn, this molecular motion impacts the high temperature photophysical properties of $\mathbf{D_{CH2Cl2}}$ in the solid state. Likely, some atomic motions in the excited states and some vibrational modes that are hindered in $\mathbf{D_{dry}}$ at RT due to its intrinsic rigidity can in this case be active and modify at high temperature the radiative and non-radiative des-excitation processes in $\mathbf{D_{CH2Cl2}}$ compared to $\mathbf{D_{dry}}$, resulting in significantly larger for RT k_{nr} non-radiative rate constant values for $\mathbf{D_{CH2Cl2}}$ compared to $\mathbf{D_{dry}}$ (Table 1). Notably, at high temperature, the red-shift of the $\mathbf{D_{CH2Cl2}}$ large emission band compared to $\mathbf{D_{dry}}$ one supports this assumption of an impact of the solid-state mobility of the included solvent molecules in the photophysics of $\mathbf{D_{CH2Cl2}}$. Indeed, such molecular motion in the solid state activates vibrational sub-levels in the different energy states that operate in the radiative relaxation processes. Once the temperature decreases, the solvent's mobility within $\mathbf{D_{CH2Cl2}}$ progressively vanishes. It results in a lower accessibility of the higher energy vibrational states inducing the blue shift observed.[15] Consequently, $\mathbf{D_{CH2Cl2}}$ presents at low temperature an emission spectrum comparable to the low temperature emission spectrum of $\mathbf{D_{dry}}$ in which these vibrational modes do not exist. The occurrence of a luminescent vapochromic behavior in $\mathbf{D_{dry}}$ is a priori quite unexpected considering its solid-state crystal structure (Fig. 1 and 2) which presents only a very low porosity associated with voids (Fig. 2d) that are not interconnected. Nevertheless, single crystals of $\mathbf{D_{dry}}$ can reversibly uptake CH_2Cl_2 vapors in a SC-SC transformation leading to the formation of 1D channels (Fig. 2e) in $\mathbf{D_{CH2Cl2}}$ single crystals, concomitantly with a luminescence vapochromic response. Very likely, the voids observed in $\mathbf{D_{dry}}$ are sufficient to allow the initiation of volatile molecules uptake process, activating a molecular motion within the single crystals. Concomitantly to this CH_2Cl_2 inclusion, the photophysical properties of the solid are altered by this molecular motion, originating the vapochromic behavior via a unique temperature dependent dynamic process. In line with this assumption, the RT k_{nr} value of $\mathbf{D_{dry}}$ ($2.1*10^4$ s^{-1}, table 1) is the lowest among all the compounds measured in this study (vide infra), confirming that the non-radiative de-excitation processes present much larger amplitudes at RT in the solvated 1D-CP networks than in $\mathbf{D_{dry}}$. This observation supports the suggested mechanism of vapochromic luminescence. Interestingly, Perruchas *et al.* recently suggested that solid-state molecular motion induced by solvent adsorption can impact the photophysics of a Cu(I) discrete assembly within porous molecular solids.[3b] This sets this 1D-CP derivative apart of the other Cu(I) based luminescent vapochromic derivatives for which intrinsic significant porosity was demonstrated to be a key preliminary factor allowing volatile molecule detection.[16] In a more general point of view, it reveals that solid-state luminescent molecular materials bearing very low porosity have to be considered as good candidates for such detection application.

Importantly, this reversible luminescence vapochromic uptake process is not limited to CH_2Cl_2 vapors but is also observed upon exposure of $\mathbf{D_{dry}}$ to EtOH, CH_3NO_2 and THF vapors, affording single crystals of $\mathbf{D_{EtOH}}$, $\mathbf{D_{CH3NO2}}$ and $\mathbf{D_{THF}}$, respectively.[7] In each case, X-ray single crystal structure analyses revealed (Fig. 4), similarly to $\mathbf{D_{CH2Cl2}}$, an uptake process associated with an increase of the unit cell volume. Within these new derivatives, included disordered solvent molecules (one and a half, one, and one molecule(s) per Cu(I) bimetallic unit in $\mathbf{D_{EtOH}}$, $\mathbf{D_{CH3NO2}}$, and $\mathbf{D_{THF}}$ respectively) are found formally located at the place of the void observed in $\mathbf{D_{dry}}$.[7] Concomitantly, the solid-state emission properties of these new phases are also altered compared to those of $\mathbf{D_{dry}}$. Indeed, as in the case of $\mathbf{D_{CH2Cl2}}$, their RT emission spectrum recorded with excitation at 370 nm are all red-shifted compared to $\mathbf{D_{dry}}$. They are characterized by a broad and featureless band having emission maximum λ_{max} at 512, 522, and 528 nm for$\mathbf{D_{EtOH}}$, $\mathbf{D_{CH3NO2}}$, and $\mathbf{D_{THF}}$, respectively (Fig. 3), typical of green-yellow to yellow eye-perceived luminescences. The RT EQY is 7 % for all these three new solvated phases. Once the source of vapor of solvent molecules is removed, these single crystals returned rapidly to the initial pale blue-cyan luminescent single crystals of $\mathbf{D_{dry}}$, revealing a general reversible luminescence vapochromic behaviour whose luminochromic signature is formally characteristic of the nature of the volatile solvent molecule used. The photophysical study[7] of these three new solvated phases reveals that $\mathbf{D_{CH3NO2}}$ and $\mathbf{D_{THF}}$ present thermal variations of their emission spectra and average emission decay lifetime (τ_{80K} = 430 μs; τ_{300K} = 8 μs for $\mathbf{D_{CH3NO2}}$ and (τ_{80K} = 692 μs; τ_{300K} = 13 μs for $\mathbf{D_{THF}}$) that are similar to those observed with $\mathbf{D_{CH2Cl2}}$.[7] Therefore, for these volatile molecules, the uptake process and its impact on the photophysical properties should proceed

accordingly to the same mechanism. The slight but human-eye detectable differences observed in the emission spectra at room temperature must be related to subtle differences in the mobility of the included molecules and their interaction with the 1D-CPs backbones. Conversely, $\mathbf{D_{EtOH}}$ presents temperature dependences of its photophysical data that are different of those of $\mathbf{D_{CH2Cl2}}$, $\mathbf{D_{CH3NO2}}$ and $\mathbf{D_{THF}}$ (Fig. 4d). Indeed, in the thermal variation of $\mathbf{D_{EtOH}}$ emission spectra, upon cooling from 300 K to 150 K, a slight bathochromic shift of the large emission band is first displayed from λ_{max} = 512 nm (300 K) to λ_{max} = 531 nm (150 K). Concomitantly, a slight increase of the intensity of the signal is observed. Then, from 150 K to 80 K, the intensity of the spectrum increases significantly accompanied by the rise of the vibronic progression assignable to ligand-centered transitions. It leads at 80 K to a large band bearing three maxima at 442 nm, 471 nm and 488 nm presenting therefore a very similar energy pattern than the other low temperature emission spectra recorded in the series, yet having a clearly different maxima intensity distribution. In addition to the bathochromic shift of the large emission band observed from 300 K to 150 K, the discrepancy of photophysics of this phase compared to the other solvated phases is also confirmed by the temperature dependence of the average emission decay lifetime for $\mathbf{D_{EtOH}}$ and its RT k_{nr} value (Table 1). Indeed, the thermal variation observed for the average emission decay lifetime presents a much more moderated amplitude (τ_{80K} = 62 μs; τ_{300K} = 3 μs for $\mathbf{D_{EtOH}}$) while the RT k_{nr} value of $\mathbf{D_{EtOH}}$ is one order magnitude larger than those of the other solvates recorded in this study. The high temperature data are typical of a TADF from the ^{1}MLCT excited state while the low temperature regime would originate from low lying ^{3}MLCT excited state operating once the solvent mobility within the crystals has significantly vanished. Such a specific behaviour in the case of the luminescent vapochromic response of $\mathbf{D_{dry}}$ in the presence of vapors of EtOH may be related to the possibility offered by this solvent to supply strong hydrogen bonds once uptake within single crystals in which semi-bridging aqua ligands are connected to Cu(I) metal centers. Yet, since the semi-bridging aqua ligands are not located in the crystal structures in the close vicinity of the voids (Fig. 2b), this effect can be mediated through indirect H-F interactions via the hexafluorophosphate anions that are closely connected to the semi-bridging aqua ligands (Fig. 1a) and might involve manifold mechanisms such as modification of the vibrational structure and reorganisation of the electronic structure in the excited states. Anyhow, the specific impact of the EtOH molecules inclusion on these 1D-CP single crystals photophysical properties reveals that the vapochromic behavior of the derivative $\mathbf{D_{dry}}$ can be associated with different temperature dependent luminescence signatures considering the family of volatile molecules investigated.

Conclusions

With these results, the interest of the [$Cu_2(\mu_2$-dppm$)_2$] units for the preparation of new multifunctional luminescent Cu(I) assemblies is confirmed and the perspectives of applications of the resulting materials are enlarged. The conformational flexibility of such Cu(I) bimetallic precursors allows the preparation of the new solid-state luminescent 1D-CPs $\mathbf{D_{dry}}$ in which a water molecule is trapped between the two Cu(I) metal centers, affording the first example of a bimetallic Cu(I) derivative bearing a semi-bridging aqua ligand. This reveals also that the conformational flexibility allowed in such bimetallic units can lead to original reactivity and new molecular materials. Importantly, in spite of their intrinsic very low porosity, single crystals of $\mathbf{D_{dry}}$ can undergo CH_2Cl_2, EtOH, CH_3NO_2 and THF vapor uptake along SC-SC transitions that display reversible luminescence vapochromic responses. Detailed temperature dependant photophysical studies conducted on the full series of solvated and non-solvated molecular solids reveal that such vapochromic behaviour are related to molecular motion of the solvent molecules occurring along 1D channels formed within the solvated crystalline solids. While a specific temperature dependant behaviour is observed with the samples submitted to EtOH vapors suggesting a special sensitivity toward hydrogen bond donors molecules, this survey also importantly highlights the complexity of the relaxation processes that may occur in such heteroleptic intricate Cu(I) supramolecular assemblies. This complexity contrasts with the simplicity of the syntheses conducted in one step under ambient conditions from cheap and easily available molecular precursors. By varying the nature of the diphosphane assembling ligands and of the polytopic cyano-capped linkers, a general and rational access to original Cu(I) supramolecular assemblies displaying original RT solid state photophysical properties can be therefore anticipated.

Conflicts of interest

There are no conflicts to declare.

Acknowledgements

This work was supported by the ANR (P-OPTOELECTR-MOLMAT), the French Research Ministry and the CNRS. C.L. thanks the Alexander von Humboldt Foundation for a fellowship for experienced researcher. Computations were performed using HPC resources from GENCI-CINES/IDRIS (Grants A0060800649 and A0080800649). The authors would like to greatly acknowledge the referees for their very valuable critical analysis of this article, in particular in relation with the interpretation of the intricate photophysical properties of the reported derivatives.

Notes and references

1 (a) V. W.-W. Yam, V. K.-M. Au and S. Y.-L. Leung, Light-Emitting Self-Assembled Materials Based on d^8 and d^{10} Transition Metal Complexes, *Chem. Rev.*, 2015, **115**, 7589–7728; (b) M.L. Saha, X. Yan and P.J. Stang, Photophysical Properties of Organoplatinum(II) Compounds and Derived Self-Assembled Metallacycles and Metallacages:

Fluorescence and its Applications, *Acc. Chem. Res.*, 2016, **49**, 2527−2539; (c) C. Bizzarri, E. Spuling, D. M. Knoll, D. Volz and S. Bräse, Sustainable Metal Complexes for Organic Light-Emitting Diodes(OLEDs), *Coord. Chem. Rev.*, 2018, **373**, 49−82.; (d)W. P. Lustig, J. Li, Luminescent metal–organic frameworks and coordination polymers as alternative phosphors for energy efficient lighting devices, *Coord. Chem. Rev.*, 2018, **373**, 116–147; (e) I. O. Koshevoy, M. Krause and A. Klein, Non-covalent intramolecular interactions through ligand-design promoting efficient photoluminescence from transition metal complexes, *Coord. Chem. Rev.*, 2020, **405**, 213094–213110; (f) D. R. Martir, E. Zysman-Colman, Photoactive Supramolecular Cages Incorporating Ru(II) and Ir(III) Metal Complexes, *Chem. Commun.*, 2019, **55**, 139–158; (g) J.-L. Zhu, L. Xu, Y.-Y. Ren, Y. Zhang, X. Liu, G.-Q. Yin, B. Sun, X. Cao, Z. Chen, X.-L. Zhao, H. Tan, J. Chen, X. Li and H.-B. Yang, Switchable Organoplatinum Metallacycles with High Quantum Yields and Tunable Fluorescence Wavelenghts, *Nature Communications*, 2019, **10**, 4285–4297; **(h)** S. Sinn, I. Yang, F. Biedermann, D. Wang, C. Kübel, J. J. L. M. Cornelissen and L. De Cola, Templated Formation of Luminescent Virus-like Particles by Tailor-made Pt (II)-Amphiphiles, *J. Am. Chem. Soc.*, 2018, **140**, 2355–2362; (i) Y.-S. Wong, M.-C. Tang, M. Ng and V. W.-W. Yam, Toward the Design of Phosphorescent Emitters of Cyclometalated Earth-Abundant Nickel(II) and Their Supramolecular Study, *J. Am. Chem. Soc.*, 2020, **142**, 7638-7346; (j) M. H.-Y. Chan, S. Y.-L. Leung and V. W.-W. Yam, Rational Design of Multi-Stimuli-Responsive Scaffolds: Synthesis of Luminescent Oligo(ethynylpyridine)-Containing Alkynylplatinum(II) Polypyridine Foldamers Stabilized by Pt···Pt Interactions, *J. Am. Chem. Soc.*, 2019, **141**, 12312–12321; (k) M.-Y. Leung, M.-C. Tang, W.-L. Cheung, S.-L. Lai, M. Ng, M.-Y. Chan and V. W.-W. Yam, Thermally Stimulated Delayed Phosphorescence (TSDP)-Based Gold(III) Complexes of Tridentate Pyrazine-Containing Pincer Ligand with Wide Emission Color Tunability and Their Application in Organic Light-Emitting Devices, *J. Am. Chem. Soc.*, 2020, **142**, 2448–2459.

2 (a) R. Czerwieniec, M. J. Leitl, H.H.H. Homeier and H. Yersin**,** Cu(I) complexes – Thermally activated delayed fluorescence. Photophysical approach and material design, *Coord. Chem. Rev.*, 2016, **325**, 2–28; (b) A. Kobayashi, M. Kato, Stimuli-responsive Luminescent Copper(I) Complexes for Intelligent Emissive Devices, *Chemistry Letters*, 2017, **46**, 154–162; (c) K. Tsuge, Y. Chishina, H. Hashiguchi, Y. Sasaki, M. Kato, S. Ishizaka and N. Kitamura, Luminescent Copper(I) Complexes with Halogenido-Bridged Dimeric Core, *Coord. Chem. Rev.*, 2016, **306**, 636−651.

3 (a) T. Hayashi, A. Kobayashi, H. Ohara, M. Yoshida, T. Matsumoto, H.-C. Chang and M. Kato, Vapochromic Luminescence and Flexibility Control of Porous Coordination Polymers by Substitution of Luminescent Multinuclear Cu(I) Cluster Nodes, *Inorg. Chem.*, 2015, **54**, 8905–8913; (b) Q. Benito, C. M. Balogh, H. E. Moll, T. Gacoin, M. Cordier, A. Rakhmatullin, C. Latouche, C. Martineau-Corcos and S. Perruchas, Luminescence Vapochromism of a Dynamic Copper Iodide Mesocate, *Chem. Eur.J.*, 2018, **24**, 18868–18872; (c) T. Hasegawa, A. Kobayashi, H. Ohara, M. Yoshida and M. Kato, Emission Tuning of Luminescent Copper(I) Complexes by Vapor-Induced Ligand Exchange Reactions, *Inorg. Chem.*, 2017, **56**, 4928–4936; (d) Z.-C. Shi, W. Chen, S.-Z. Zhan, M. Li, M. Xie, Y. Y. Li, S. W. Ng, Y.-L. Huang, Z. Zhang, G.-H. Ning and D. Li, Guest Effects on Crystal Structure and Phosphorescence of a Cu_6L_3 Prismatic Cage, *Inorg. Chem. Front.*, 2020,**7**, 1437–1444; (e) J. Nitsch, F. Lacemon, A. Lorbach, A. Eichhorn, F. Cisnetti and A. Steffen, Cuprophilic interactions in highly luminescent dicopper(I)–NHC–picolyl complexes – fast phosphorescence or TADF?, *Chem. Commun.*, 2016, **52**, 2932–2935; (f) B. Hupp, J. Nitsch, T. Schmitt, R. Bertermann, K. Edkins, F. Hirsch, I. Fischer, M. Auth, A. Sperlich and A. Steffen, Stimulus-Triggered Formation of an Anion–Cation Exciplex in Copper(I) Complexes as a Mechanism for Mechanochromic Phosphorescence, *Angew. Chem. Int. Ed.,* **2018**, ***57***, 13671–13675; (g) B. Hupp, C. Schiller, C. Lenczyk, M. Stanoppi, K. Edkins, A. Lorbach and A. Steffen, Synthesis, Structures, and Photophysical Properties of a Series of Rare Near-IR Emitting Copper(I) Complexes, *Inorg. Chem.,* **2017**, ***56***, 8996–9008; (h) G. Chakkaradhari, Y.-T. Chen, A. J. Karttunen, M. T. Dau, J. Jänis, S. P. Tunik, P.-T. Chou, M.-L. Ho and I. O. Koshevoy, Luminescent Triphosphine Cyanide d^{10} Metal Complexes *Inorg. Chem.,* **2016**, ***55***, 2174-2184*;* (i) R. Hamze, J. L. Peltier, D. Sylvinson, M. Jung, J. Cardenas, R. Haiges, M. Soleilhavoup, R. Jazzar, P. I. Djurovich, G. Bertrand and M. E. Thompson, Eliminating nonradiative decayin Cu(I) emitters: >99% quantum efficiency and microsecond lifetime, *Science.*, 2019, **363**, 601–606; (j) S. Shi, M. C. Jung, C. Coburn, A. Tadle, M. R. D. Sylvinson, P. I. Djurovich, S. R. Forrest and M. E. Thompson, Highly Efficient Photo- and Electroluminescence from Two-Coordinate Cu(I) Complexes Featuring Nonconventional N-Heterocyclic Carbenes, *J. Am. Chem. Soc.*, 2019, **141**, 3576–3588; (k) A. S. Romanov, D. Di, L. Yang, J. Fernandez-Cestau, C. R. Becker, C. E. James, B. Zhu, M. Linnolahti, D. Credgington and M. Bochmann, Highly Photoluminescent Copper Carbene Complexes Based on Prompt Rather Than Delayed Fluorescence, *Chem.Commun.*, 2016, **52**, 6379–6382; (l) M. Mohankumar, F. Monti, M. Holler, F. Niess, B. Delavaux-Nicot, N. Armaroli, J.-P. Sauvage and J.-F. Nierengarten, Combining Topological and Steric Constraints for the Preparation of Heteroleptic Copper(I) Complexes, *Chem. Eur. J.*, 2014, **20**, 12083–12090; (m) M. J. Leitl, V. A. Krylova, P. I. Djurovich, M. E. Thompson and H. Yersin, Phosphorescence Versus Thermally Activated Delayed Fluorescence. Controlling Singlet-Triplet Splitting in Brightly Emitting and Sublimable Cu(I) Compounds, *J. Am. Chem. Soc.*, 2014, **136**, 16032–16038; (n) S. Keller, A. Prescimone, H. Bolink, M. Sessolo, G. Longo, L. Martínez-Sarti, J. M. Junquera-Hernández, E. C. Constable, E. Ortí and C. E. Housecroft, Luminescent Copper(I) Complexes with Bisphosphane and Halogen-Substituted 2,2'-Bipyridine Ligands, *Dalton Trans.*, 2018, **47**, 14263−14276; (o) C. M. Brown, C. Li, V. Carta, W. Li, Z. Xu, P. H. F. Stroppa, I. D. W. Samuel, E. Zysman-Colman and M. O. Wolf, Influence of Sulfur Oxidation State and Substituents on Sulfur-Bridged Luminescent Copper(I) Complexes Showing Thermally Activated Delayed Fluorescence, *Inorg. Chem.*, 2019, **58**, 7156−7168; (p) S. Perruchas, X. F. Le Goff, Maron, S. I. Maurin, F. Guillen, A. Garcia, T. Gacoin and J.-P. Boilot, Mechanochromic and Thermochromic Luminescence of a Copper Iodide Cluster, *J. Am. Chem. Soc.*, 2010, **132**, 10967−10969; (q) Q. Benito, X. F. Le Goff, S. Maron, A. Fargues, A. Garcia, C. Martineau, F. Taulelle, S. Kahlal, T. Gacoin, J.-P. Boilot and S. Perruchas, Polymorphic Copper Iodide Clusters: Insights into the Mechanochromic Luminescence Properties, *J. Am. Chem. Soc.*, 2014, **136**, 11311–11320; (r) B. Huitorel, H. El Moll, R. Utrera-Melero, M. Cordier, A. Fargues, A. Garcia, F. Massuyeau, C. Martineau-Corcos, F. Fayon, A. Rakhmatullin, S. Kahlal, J.-Y. Saillard, T. Gacoin and S. Perruchas, Evaluation of Ligands Effect on the Photophysical Properties of Copper Iodide Clusters*, Inorg. Chem.,* 2018*,* **57**, 4328–4339; (s) A. Kobayashi, Y. Yoshida, M. Yoshida and M. Kato, Mechanochromic Switching between Delayed Fluorescence and Phosphorescence of Luminescent Coordination Polymers Composed of Dinuclear Copper(I) Iodide Rhombic Cores, *Chem. Eur. J.*, 2018, **24**, 14750–14759; (t) A. Kobayashi, M. Fujii, Y. Shigeta, M. Yoshida and M. Kato, Quantitative Solvent-Free Thermal Synthesis of Luminescent Cu(I)

Coordination Polymers, *Inorg. Chem.*, 2019, **58**, 4456–4464; (u) S.–S. Zhao, L. Wang, Y. Liu, L. Chen and Z. Xie, Stereochemically Dependent Synthesis of Two Cu(I) Cluster-Based Coordination Polymers with Thermochromic Luminescence, *Inorg. Chem.*, 2019, **58**, 4456–4464; (w) A. V. Artem'ev, M. R. Ryzhikov, I. V. Taidakov, M. I. Rakhmanova, E. A. Varaksina, I. Y. Bagryanskaya, S. F. Malysheva and N. A. Belogorlova, Bright green-to-yellow emitting Cu(I) complexes based on bis(2-pyridyl)phosphine oxides: synthesis, structure and effective thermally activated-delayed fluorescence, *Dalton Trans.*, 2018, **47**, 2701–2710; (x) A. V. Artem'ev, E. A. Pritchina, M. I. Rakhmanova, N. P. Gritsan, I. Y. Bagryanskaya, S. F. Malysheva and N. A. Belogorlova, Alkyl-dependent self-assembly of the first red-emitting zwitterionic $\{Cu_4I_6\}$ clusters from $[alkyl\text{-}P(2\text{-}Py)_3]^+$ salts and CuI: when size matters, *Dalton Trans.*, 2019, **48**, 2328–2337; (y) A. Y. Baranov, A. S. Berezin, D. G. Samsonenko, A. S. Mazur, P. M. Tolstoy, V. F. Plyusnin, I. E. Kolesnikov and A. V. Artem'ev, New Cu(I) halide complexes showing TADF combined with room temperature phosphorescence: the balance tuned by halogens, Dalton Trans., 2020, **49**, 3155–3163.

4 (a) A. Kobayashi, R. Arata, T. Ogawa, M. Yoshida and M. Kato, Effect of Water Coordination on Luminescent Properties of Pyrazine-Bridged Dinuclear Cu(I) Complexes, *Inorg. Chem.*, 2017, **56**, 4280−4288; (b) J. P. Naskar, S. Chowdhury, M. G. B. Drew and D. Datta, Chemistry of the copper(I)–water bond. Some new observations, *New J. Chem.*, 2002, **26**, 170–175; (c) A. G. P. Gutiérrez, J. Zeitouny, A. Gomila, B. Douziech, N. Cosquer, F. Conan, O. Reinaud, P. Hapiot, Y. Le Mest, C. Lagrost and N. Le Poul, Insights into water coordination associated with the Cu^{II}/Cu^{I} electron transfer at a biomimetic Cu centre, *DaltonTrans.*,2014, **43**, 6436–6445; (d) M. Munakata, S. Kitagawa, N. Ujimaru, M. Nakamura, M. Maekawa and H. Matsuda, Synthesis, structures, and properties of the molecular assemblies of copper(I) and silver(I) complexes with phenazine. Novel donor-acceptor and huge polynuclear complexes, *Inorg. Chem.*, 1993, **32**, 826–832; (e) M. M. Olmstead, W. K. Musker and R. M. Kessler, Differences in the coordinating ability of water, perchlorate and tetrafluoroborate toward copper(I). The X-ray crystal structures of $[Cu(1,4\text{-thioxane})_3OClO_3]$, $[Cu(1,4\text{-thioxane})_3OH_2]BF_4$ and $[Cu(1,4\text{-thioxane})_4BF_4$, *Transition Met. Chem.*, 1982, **7**, 140–146.

5 B. Nohra, Y. Yao, C. Lescop and R. Réau, Coordination Polymers with π-Stacked Metalloparacyclophane Motifs: F-Shaped Mixed-Coordination Dinuclear Connectors, *Angew. Chem. Int. Ed.*, 2007, **46**, 8242–8245.

6 (a) C. Lescop, Coordination-Driven Syntheses of Compact Supramolecular Metallacycles toward Extended Metallo-organic Stacked Supramolecular Assemblies, *Acc. Chem. Res.*, 2017, ***50***, 885–894; (b) B. Nohra, E. Rodriguez-Sanz, C. Lescop and R. Réau, Chemistry of Bridging Phosphanes: Cu^{I} Dimers Bearing 2,5-Bis(2-pyridyl)phosphole Ligands, *Chem. Eur. J.*, 2008, **14**, 3391–3403; (c) A. I. Aranda Perez, T. Biet, S. Graule, T. Agou, C. Lescop, N. R. Branda, J. Crassous and R. Réau, Chiral and Extended π-Conjugated Bis(2-pyridyl)phospholes as Assembling N,P,N Pincers for Coordination-Driven Synthesis of Supramolecular [2,2]Paracyclophane Analogues, *Chem. Eur. J.*, 2011, **17**, 1337-1351.

7 For experimental details, spectroscopic, X-ray diffraction data and computational studies, see SI.

8 The void volumes were estimated using the PLATON SQUEEZE program: (a) A. L. Spek, Single-crystal structure validation with the program PLATON, *J. Appl. Crystallogr.*, 2003, **36**, 7–13; (b) P. van der Stuis, A. L. Spek, BYPASS: an effective method for the refinement of crystal structures containing disordered solvent regions, *Acta Crystallogr.*, 1990, **46**, 194–201.

9 a research on the CCDC using the fragment entry Cu(+1)-OH_2-Cu(+1) afforded 72 results that all revealed to be Cu(II) polymetallic derivatives

10 The vertical electronic excitation energies of the first vertical singlet and triplet excited states were calculated by time-dependant DFT protocol. A complete study would imply geometry optimizations of the excited states to be comparable to the emission experimental data. This would necessitate taking into account the polymer and crystal reorganisation relaxations that constrain the molecular unit which is not possible at this molecular level of simulation.

11 These temperature dependant behaviour are not dependant of the excitation energy and similar results were obtained with (λ_{ex} = 330 nm), see SI.

12 (a) M. El Sayed Moussa, S. Evariste, H.-L. Wong, L. Le Bras, C. Roiland, L. Le Polles, B. Le Guennic, K. Costuas, V. W.-W. Yam and C. Lescop, A solid state highly emissive Cu(I) metallacycle: promotion of cuprophilic interactions at the excited states, *Chem. Comm*., 2016, **52**, 11370–11373; (b) S. Evariste, A. M. Khalil, M. El Sayed Moussa, A. K.-W. Chan, E. Y.-H. Hong, H.-L. Wong, B. Le Guennic, G. Calvez, K. Costuas, V. W.-W. Yam and C. Lescop, Adaptive Coordination-Driven Supramolecular Syntheses toward New Polymetallic Cu(I) Luminescent Assemblies. *J. Am. Chem. Soc.,* 2018, **140**, 12521–12526; (c) M. El Sayed Moussa, A. M. Khalil, S. Evariste, H.-L. Wong, V. Delmas, B. Le Guennic, G. Calvez, K. Costuas, V.-W. Yam and C. Lescop, Intramolecular rearrangements guided by adaptive coordination-driven reactions toward highly luminescent polynuclear Cu(I) assemblies, *Inorg. Chem. Front.*, 2020, **7**, 1334–1344; (d) S. Evariste, M. E. S. Moussa, H.-L. Wong, G. Calvez, V.-W. Yam and C. Lescop, Straightforward Preparation of a Solid-state Luminescent Cu-11 Polymetallic Assembly via Adaptive Coordination-driven Supramolecular Chemistry, *Z. Anorg. Allg. Chem.*, 2020, 646, 754-760.

13 This unusual behaviour recorded for the thermal variation of the average emission decay lifetime τ of $\mathbf{D_{dry}}$ was confirmed by several measurements performed on different and independent batches of the derivative $\mathbf{D_{dry}}$. See for another example fig. S17

14 Highly Efficient OLEDs Materials Based on Thermally Activated Delayed Fluorescence, ed. H. Yersin, Wiley-VCH, Weinheim, 2019.

15 (a) Y. Zhang, M. Schulz, M. Wächtler, M. Karnahl and B. Dietzek, Heteroleptic diamine-diphosphone Cu(I) complexes as an alternative towards noble-metal based photosensitizers: design strategies, photophysical properties and perspective applications, *Coord. Chem. Rev.*, 2018, **356**, 127-146; (b) R. Czerwieniec and H. Yersin, Diversity of copper(I) complexes showing thermally activated delayed fluorescence: basic photophysical analysis, *Inorg. Chem.*, 2015, **54**, 4322-4327.

16 Note that this blue shift at low temperature has also a contribution resulting from increased bulk rigidity at low temperature that leads to overall smaller excited state distortion (general rigidochromic effect).

17 F. Biedermann, L. De Cola, Porous supramolecular materials: the importance of emptiness, *Supramolecular Chemistry*, 2018, **30**, 166–168.